

# Pharmacological Properties and Physiological Function of a P2X-Like Current in Single Proximal Tubule Cells Isolated from Frog Kidney

John P. Davies · Louise Robson

Received: 22 July 2010 / Accepted: 22 September 2010 / Published online: 23 October 2010  
© The Author(s) 2010. This article is published with open access at Springerlink.com

**Abstract** Although previous studies have provided evidence for the expression of P2X receptors in renal proximal tubule, only one cell line study has provided functional evidence. The current study investigated the pharmacological properties and physiological role of native P2X-like currents in single frog proximal tubule cells using the whole-cell patch-clamp technique. Extracellular ATP activated a cation conductance ( $P2X_f$ ) that was also  $Ca^{2+}$ -permeable. The agonist sequence for activation was  $ATP = \alpha\beta\text{-MeATP} > \text{BzATP} = 2\text{-MeSATP}$ , and  $P2X_f$  was inhibited by suramin, PPADS and TNP-ATP. Activation of  $P2X_f$  attenuated the rundown of a quinidine-sensitive  $K^+$  conductance, suggesting that  $P2X_f$  plays a role in  $K^+$  channel regulation. In addition, ATP/ADP apyrase and inhibitors of  $P2X_f$  inhibited regulatory volume decrease (RVD). These data are consistent with the presence of a P2X receptor that plays a role in the regulation of cell volume and  $K^+$  channels in frog renal proximal tubule cells.

**Keywords** Purinergic receptor physiology in epithelia · Renal physiology · Ion channel · Potassium ion channel · Volume regulation in epithelial cells

**Electronic supplementary material** The online version of this article (doi:10.1007/s00232-010-9308-8) contains supplementary material, which is available to authorized users.

J. P. Davies · L. Robson (✉)  
Department of Biomedical Science, University of Sheffield,  
Sheffield S10 2TN, UK  
e-mail: l.robson@sheffield.ac.uk

## Introduction

P2 purinoceptors are a class of ATP-activated receptors that play a critical role in a variety of cellular processes in both electrically excitable and nonexcitable cells. They are subdivided into two distinct classes, P2X and P2Y receptors (Burnstock and Kennedy 1985; North and Barnard 1997). P2X receptors are ATP-gated, nonselective,  $Ca^{2+}$ -permeable cation channels that, on activation, allow extracellular  $Ca^{2+}$  to enter the cell, leading to a rise in intracellular  $Ca^{2+}$ . The P2Y receptors are G protein-coupled. On activation, some P2Y receptors cause a rise in intracellular  $Ca^{2+}$ , via the release of  $Ca^{2+}$  from intracellular stores.

At the molecular level a number of mammalian P2X and P2Y receptors have been identified,  $P2X_{1-7}$  and  $P2Y_{1,2,4,6,11-14}$ , with only two amphibian P2X receptors identified,  $P2X_4$  (Juranka et al. 2001) and a  $P2X_5$ -like current (Jensik et al. 2001). These receptors can act as homomeric channels and form heteromeric channels. To date, in heterologous systems, combinations of a number of P2X receptors have been observed, including  $P2X_{2/3}$ ,  $P2X_{1/5}$  and  $P2X_{4/6}$  (Le et al. 1998, 1999; Radford et al. 1997; Torres et al. 1999). There is also evidence for the presence of  $P2X_{2/3}$  heteromers in rat nodose neurons (Lewis et al. 1995). A more recent study has provided evidence for  $P2X_{4/7}$  receptors (Guo et al. 2007). The properties of these heteromers are determined by their receptor composition, with properties taken from both receptor types. This means that heteromeric channels demonstrate very different properties from the single cloned receptors.

Both P2X and P2Y family members are found in the kidney, with the majority of work on renal P2 receptors to date focusing on their role in the distal tubule and collecting duct. Previous work has demonstrated that both

P2X and P2Y receptors regulate the activity of the epithelial  $\text{Na}^+$  channel (ENaC). P2Y<sub>2</sub> receptors inhibit ENaC function (Pochynyuk et al. 2008), while basolateral P2X<sub>4</sub> and heteromeric P2X<sub>4/6</sub> have been shown to activate ENaC (Wildman et al. 2008; Zhang et al. 2007). In inner medullary collecting duct cells there is evidence for a role for P2X<sub>1</sub>, P2X<sub>3</sub>, P2X<sub>4</sub>, P2Y<sub>1</sub> and P2Y<sub>2</sub> (McCoy et al. 1999; Xia et al. 2004) in regulating  $\text{Na}^+$  and  $\text{Cl}^-$  transport. In addition, P2 receptors regulate aquaporin-2-mediated water reabsorption and  $\text{K}^+$  channel activity in the collecting duct (Lu et al. 2000; Wildman et al. 2009). In the thick ascending limb P2 receptors also play a regulatory role, with P2Y<sub>2</sub> and an as yet unidentified P2X receptor involved (Jensen et al. 2007; Silva and Garvin 2009). P2Y<sub>2</sub> receptors are also thought to be important in macula densa cell signaling (Liu et al. 2002) and in the modulation of apoptosis of human mesangial cells (Solini et al. 2007). In the proximal tubule a significant body of work has concentrated on P2Y receptors, with molecular and functional approaches indicating the presence of P2Y<sub>1</sub>, P2Y<sub>2</sub>, P2Y<sub>4</sub> and P2Y<sub>6</sub> (Bailey 2004; Bailey et al. 2001; Cha et al. 1998; Chan et al. 1998; Lee et al. 2005). These P2Y receptors are thought to play an important role in regulating  $\text{Na}^+$ -glucose transport activity,  $\text{HCO}_3^-$  reabsorption and the regulation of basolateral  $\text{Cl}^-$  channels (Bailey et al. 2001; Bouyer et al. 1998; Lee et al. 2005). In contrast, very few studies have identified P2X receptors at either the molecular or the functional level in proximal tubule. The few studies completed have used cell lines and primary cultures and provide evidence for the expression of P2X<sub>1</sub>, P2X<sub>4</sub>, P2X<sub>5</sub> and P2X<sub>6</sub> (Filipovic et al. 1998; Leipziger and Unwin 2003; Takeda et al. 1998). At a functional level, only studies in LLC-PK<sub>1</sub> cells have shown ATP-activated, P2X-mediated currents (Filipovic et al. 1998). In these cells, the pharmacological properties of the current were consistent with P2X<sub>2</sub>, although RT-PCR identified a fragment that closely resembled rat P2X<sub>1</sub>. To date, no study has shown evidence for the existence of functional P2X receptors in native proximal tubule cells. Therefore, the aim of the current study was to examine the physiological function and pharmacological properties of an ATP-activated current in freshly isolated frog single proximal tubule cells.

## Methods

### Cell Isolation

Single proximal tubule cells were isolated from *Rana temporaria* using an enzyme digestion technique (Hunter 1989). Frogs were killed by stunning, and the brain and spinal cord were destroyed prior to removal of the kidneys, in accordance with U.K. legislation. Proximal tubule cells

were identified by their “snowman” appearance (Robson and Hunter 1994c).

### Cell Length Experiments

Cell length was measured using two different techniques that utilize changes in light intensity at the cell membrane/bath interface. The first technique used a photodiode array-based system as described previously (Mounfield and Robson 1998), while the second technique used a digital camera-based system (Soft Cell; Cairn Research, Kent, UK). Cells were initially superfused with frog Ringer that contained (in mM) 50 NaCl, 3 KCl, 2 CaCl<sub>2</sub>, 1 MgCl<sub>2</sub>, 10 HEPES (titrated to pH 7.4 using NaOH) and 89 mannitol. Hypotonic shock was then induced by the removal of 40 mM mannitol. This was repeated in unpaired cells in the presence of varying P2X receptor antagonists (camera-based system) or in the presence of ATP/ADP apyrase (array-based system), which breaks down ATP. Thus, if ATP release is important in volume regulation, then ATP/ADP apyrase should inhibit the regulatory response. Antagonist or apyrase was present in both control and hypotonic solutions. All test solutions were compared to day-matched controls.

### Patch Experiments

Approximately 20  $\mu\text{l}$  of the cell suspension was placed in a Perspex bath on the stage of an inverted microscope (IX70; Olympus, Tokyo, Japan). Standard patch-clamp techniques were employed to investigate whole-cell currents (Hamill et al. 1981), with voltage protocols driven from a computer equipped with a Digidata interface (Axon Instruments, Foster City, CA). Data were obtained and analyzed using pClamp (Axon Instruments). Recordings were made using a List EPC-7 amplifier (HEKA, Lambrecht, Germany). On achieving the whole-cell configuration via the basolateral aspect of the cell, currents were saved directly onto the hard disk of the computer following low-pass filtering at 5 kHz. Microsoft (Redmond, WA) Excel 2000 was used to determine average steady-state currents at each potential. Cell area was calculated from the capacity transients seen in response to a 20-mV potential step, with membrane capacitance assumed to be 1  $\mu\text{F}/\text{cm}^2$ . Except where stated, the pipette contained a high- $\text{Na}^+$  solution (in mM) 100 NaCl, 2 MgCl<sub>2</sub>, 0.5 EGTA and 10 HEPES (titrated to pH 7.4 with NaOH) and the bath contained (in mM) 100 NaCl, 0.5 CaCl<sub>2</sub>, 0.5 MgCl<sub>2</sub> and 10 HEPES (titrated to pH 7.4 with NaOH). In experiments investigating the properties of the ATP-activated current, the total ATP added to the extracellular solution was adjusted to give a constant free ATP concentration between control and test conditions (Maxchelator, maxchelator.stanford.edu). For higher

concentrations of agonists, osmolality was maintained by substitution of mannitol.

Two different voltage-clamp approaches were used. In one set of experiments clamp potential was held constant at  $-100$  mV and changes in current at this potential were recorded over time. At various time points potential was ramped to between  $-100$  and  $+20$  mV. In the second set of experiments whole-cell potential was clamped at  $-40$  mV and then stepped to between  $+20$  and  $-100$  mV in  $-20$  mV steps. The reversal potential ( $V_{\text{rev}}$ ) of currents obtained using this voltage protocol was determined using polynomial regression analysis. The ATP-activated conductance ( $G_{\text{ATP}}$ ) was taken over the potential range  $-100$  to  $-20$  mV. For  $\text{K}^+$  current studies, outward ( $G_{\text{out}}$ ) and inward ( $G_{\text{in}}$ ) chord conductances were calculated from outward and inwardly directed currents, respectively.

#### *Effect of ATP and BzATP*

Patches were exposed to  $100$   $\mu\text{M}$ ,  $200$   $\mu\text{M}$ ,  $500$   $\mu\text{M}$  and  $2$  mM  $3'$ - $O$ -(4-benzoyl)benzoyl ATP (BzATP) and ATP. The order of exposure to the two agonists was varied to ensure that there was no effect of desensitization. To examine possible desensitization, whole-cell patches were exposed to an agonist (either  $2$  mM BzATP or  $500$   $\mu\text{M}$  ATP) three times. The dose response to these agonists was determined using the following bath solution (in mM):  $85$  NaCl,  $0.5$   $\text{CaCl}_2$ ,  $0.1$   $\text{MgCl}_2$ ,  $25$  mannitol and  $10$  HEPES (titrated to pH  $7.4$  with NaOH). Cells were exposed to either ATP or BzATP ( $10$ ,  $8$ ,  $4$ ,  $2$ ,  $1$  and  $0.5$  mM).

#### *Agonist Potency and Effect of Antagonists*

Patches were exposed to  $500$   $\mu\text{M}$  ATP, followed by  $500$   $\mu\text{M}$  of a second agonist, either BzATP, 2-methylthio ATP (2-MeSATP) or  $\alpha,\beta$  methylene ATP ( $\alpha\beta$ -MeATP). To examine the effect of antagonists, patches were exposed to  $500$   $\mu\text{M}$  ATP alone, then ATP in the presence of one of the following P2X receptor antagonists: suramin,  $2',3'$ - $O$ -(2,4,6-trinitrophenyl)-ATP (TNP-ATP) or pyridoxal-5-phosphate-6-azophenyl- $2',4'$ -disulfonic acid (PPADS). The effect of the P2X<sub>7</sub> antagonists brilliant blue G (BBG) (Jiang et al. 2000) and KN-62 (Humphreys et al. 1998) were examined by exposing patches to  $2$  mM BzATP and then BzATP in the presence of the antagonist.

#### *Current Properties and Relative Permeability of ATP-Activated Current*

Whole-cell patches were obtained with the standard high- $\text{Na}^+$  pipette solution. The bath contained (in mM)  $100$  NaCl,  $0.5$   $\text{CaCl}_2$ ,  $0.1$   $\text{MgCl}_2$  and  $10$  HEPES (titrated to pH  $7.4$  with NaOH). Current activation was achieved using  $2$  mM ATP.

To examine the effect of ivermectin, an antiparasitic agent known to enhance activation of P2X<sub>4</sub> (Priel and Silberberg 2004), whole-cell patches were obtained with a bath solution containing (in mM)  $20$  NaCl,  $0.5$   $\text{CaCl}_2$ ,  $0.1$   $\text{MgCl}_2$ ,  $160$  mannitol and  $10$  HEPES (titrated to pH  $7.4$  with NaOH). The effect of  $10$   $\mu\text{M}$  ivermectin was determined in paired cells, with patches exposed to  $2$  mM ATP initially and then after incubation with ivermectin for  $1$  min.

To determine the cation to anion permeability ratio, a dilution protocol was used. ATP-activated currents were recorded in paired cells in both  $100$  and  $20$  mM NaCl. Osmolality was maintained by the addition of  $160$  mM mannitol to the  $20$  mM solution. The junction potential shift induced by reducing bath NaCl fivefold was measured using a flowing  $3$  M KCl reference electrode, and all  $20$  mM NaCl  $V_{\text{rev}}$  values were corrected for this value. The monovalent cation permeability ratio was determined in paired cells by substituting  $100$  mM NaCl with either RbCl, CsCl or LiCl. To determine the relative permeability for  $\text{Na}^+$  to  $\text{NMDG}^+$ , whole-cell patches were obtained with  $100$  mM NaCl,  $0.5$  mM EGTA and  $10$  mM HEPES (titrated to pH  $7.4$  using NaOH) in the pipette and  $100$  mM NMDG-Cl and  $10$  mM HEPES (titrated to pH  $7.4$  using NMDG<sup>+</sup>) in the bath. The ATP-activated current was determined (addition of  $4$  mM ATP to the bath). To determine the  $\text{Ca}^{2+}$  to  $\text{Na}^+$  permeability ratio, the extracellular solution was then exchanged for one that contained  $5$  mM  $\text{CaCl}_2$ , in addition to NMDG-Cl and HEPES. For all permeability ratio calculations the Goldman-Hodgkin-Katz voltage equation was used, with a modified form utilized in the  $\text{Ca}^{2+}$  to  $\text{Na}^+$  calculation (Laycock et al. 2009).

#### *Effect of Extracellular Cations*

The bath contained (in mM)  $100$  NaCl and  $10$  HEPES (titrated to pH  $7.4$  with NaOH). Patches were exposed to  $2$  mM ATP under the control circumstance and then in the presence of either  $100$   $\mu\text{M}$   $\text{Zn}^{2+}$  or  $50$   $\mu\text{M}$   $\text{Cu}^{2+}$ . In  $\text{Ca}^{2+}$  experiments the effect of ATP was examined with either  $0.5$  (control) or  $2$  (test) mM  $\text{Ca}^{2+}$  in the bath. The effect of extracellular pH was examined using the standard bath solution, with patches exposed to  $2$  mM ATP at pH  $7.4$  and either pH  $6.3$  (addition of HCl) or pH  $8.3$  (addition of NaOH).

#### *Effect of P2X Activation on Whole-Cell $\text{K}^+$ Conductance*

To determine the effect of activation of the frog P2X receptor on  $\text{K}^+$  channels, whole-cell  $\text{K}^+$  currents were measured in the absence and presence of ATP. The pipette contained (in mM)  $100$  KCl,  $2$   $\text{MgCl}_2$ ,  $10$  HEPES (titrated to pH  $7.4$  with KOH) and  $0.25$  EGTA as well as  $25$  units/ml

alkaline phosphatase, which was included to reduce K<sup>+</sup> channel rundown. The bath contained (in mM) 92 NaCl, 3 KCl, 1 CaCl<sub>2</sub>, 0.5 MgCl<sub>2</sub>, 10 HEPES (titrated to pH 7.4 with NaOH) and 20 mannitol. On achieving the whole-cell configuration, 1 mM quinidine was added to the bath and the current sensitive to quinidine was taken as the magnitude of the K<sup>+</sup> currents. Quinidine has previously been shown to inhibit two K<sup>+</sup>-selective currents in frog renal proximal tubule cells (Robson and Hunter 1997). The quinidine-sensitive current was then determined again after 5 min. To examine the effect of P2X receptor activation, whole-cell patches were obtained as described previously. However, after the first exposure to quinidine and subsequent wash, cells were exposed to 4 mM ATP. ATP was left in the bath for 5 min, and the quinidine-sensitive current was determined after this time.

### Chemicals and Solutions

The osmolality of all solutions was measured (Roebeling osmometer) and adjusted to within 1 mosmol/kg water of 215 mosmol/kg water with water or mannitol as appropriate. Chemicals were obtained from Sigma (St. Louis, MO) and were of analytical grade.

### Statistics

Results are given as means  $\pm$  1 SEM, with the number of experiments in parentheses. Except where stated in the text, significance was tested using paired Student's *t*-test. Additional tests included unpaired Student's *t*-test, ANOVA, Fisher's exact probability test and correlation coefficient as appropriate. For all, significance was assumed at the 5% level.

## Results

### Effect of ATP and BzATP

Both ATP and BzATP increased whole-cell currents at  $-100$  mV, although ATP gave a greater increase compared to BzATP. ATP increased whole-cell currents at all concentrations tested ( $P \leq 0.001$  for all). BzATP increased whole-cell currents at 2 mM ( $P = 0.004$ ) and 500  $\mu$ M ( $P = 0.0004$ ) but was without effect at 200  $\mu$ M ( $P = 0.267$ ) and 100  $\mu$ M ( $P = 0.192$ ). Figure 1a, b shows typical traces from cells exposed to 500  $\mu$ M ATP. Mean agonist-activated currents are shown in Fig. 1c. At all concentrations the response to ATP was greater than the response to BzATP (unpaired Student's *t*-test). The BzATP and ATP activated current did not demonstrate desensitization. The 2 mM BzATP-activated currents were

$-12.5 \pm 1.67$ ,  $-16.0 \pm 4.52$  and  $-11.51 \pm 1.92$  pA ( $n = 13$ ) for first, second and third exposures, respectively. The mean 500  $\mu$ M ATP activated currents were  $-10.6 \pm 2.96$ ,  $-8.77 \pm 1.78$  and  $-9.08 \pm 1.23$  pA ( $n = 13$ ) for first, second and third exposures, respectively. There was no significant difference between these:  $F_{2,36} = 0.69$  and  $F_{2,36} = 0.23$ , for BzATP and ATP, respectively (ANOVAs). There was also no correlation between current activation and exposure number ( $r^2 = 0.04$  and  $r^2 = 0.08$ ).

ATP activated the whole-cell current in a dose-dependent manner (Fig. 1d). Half-maximal activation was observed with  $2.77 \pm 0.24$  mM ATP ( $n = 9$ ), with a Hill coefficient of  $3.89 \pm 0.57$  and maximal current of  $-30.1 \pm 3.68$  pA ( $r^2 = 0.992 \pm 0.002$ ). BzATP also activated the currents in a dose-dependent manner. Half-maximal activation was observed with  $4.00 \pm 0.38$  mM BzATP ( $n = 7$ ), with a Hill coefficient of  $2.00 \pm 0.07$  and maximal current of  $-32.1 \pm 2.31$  pA ( $r^2 = 0.997 \pm 0.001$ ). The ATP concentration required for half-maximal activation was significantly smaller than the half-maximal concentration of BzATP ( $P = 0.01$ , unpaired Student's *t*-test). There was no significant difference between the maximal current activated by either agonist ( $P = 0.62$ , unpaired Student's *t*-test).

### Agonist Potency and Effect of Antagonists

At 500  $\mu$ M, ATP, BzATP, 2-MeSATP and  $\alpha\beta$ -MeATP all increased whole-cell currents ( $P \leq 0.0001$ ). In paired cells the effect of ATP on whole-cell current was greater than the effect of either BzATP ( $n = 12$ ,  $P = 0.003$ ) or 2-MeSATP ( $n = 24$ ,  $P < 0.0005$ ) (Fig. 2). In contrast, ATP and  $\alpha\beta$ -MeATP increased currents by comparable amounts ( $n = 13$ ,  $P = 0.30$ ) (Fig. 2). The agonist potency sequence was ATP =  $\alpha\beta$ -MeATP > BzATP = 2-MeSATP. In the presence of 100  $\mu$ M suramin ( $n = 16$ ), 30 nM TNP-ATP ( $n = 16$ ) or 10  $\mu$ M PPDAS ( $n = 21$ ), the ATP-activated current was inhibited by 30%, 44% and 34%, respectively ( $P < 0.008$  for all) (Fig. 3). The inhibition by suramin and PPDAS was reversible, but that by TNP-ATP was not. It has previously been demonstrated that inhibition by PPDAS can be increased after incubation for 10 min. However, in paired cells the ATP-activated current in the presence of PPDAS at 1 min,  $-9.00 \pm 1.82$  pA ( $n = 9$ ), was not significantly different from that at 10 min,  $-10.2 \pm 4.12$  pA ( $n = 9$ ,  $P = 0.65$ ). PPDAS (100  $\mu$ M) inhibited the ATP-activated current by 65%,  $-11.2 \pm 1.91$  pA ( $n = 9$ ) vs.  $-3.94 \pm 1.12$  pA, in the absence and presence of PPDAS, respectively ( $P = 0.01$ ). On wash the response to ATP recovered,  $-11.1 \pm 1.64$  pA. P2X<sub>7</sub> antagonists were without effect on BzATP-activated currents. BzATP increased whole-cell current by  $-22.3 \pm 6.86$  pA ( $n = 6$ ) and  $-21.9 \pm 8.41$  pA in the absence and presence of BBG,

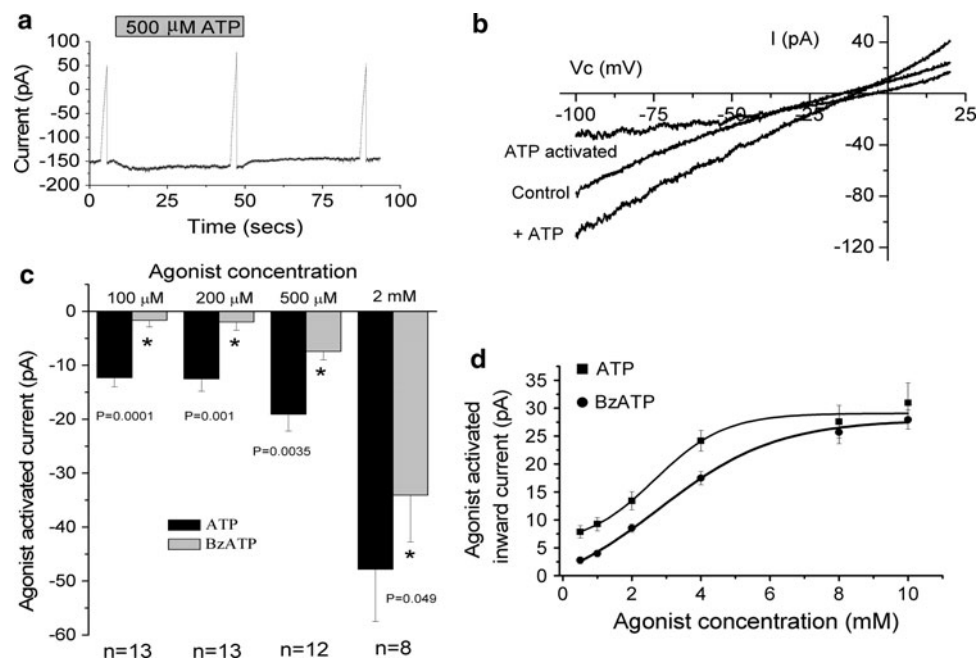


**Fig. 1** Effect of different concentrations of ATP and BzATP. Clamp potential was held at  $-100$  mV. At three time points (control, plus ATP and wash) a ramp protocol was run between  $-100$  and  $+20$  mV. **a** A typical trace (current in picoamperes against time in seconds), showing the effect of  $500$  μM ATP. Solid bar indicates when ATP was present in the bath. **b** Typical  $I$ - $V$  traces showing the current recorded under the control circumstance, in the presence of  $500$  μM ATP and the ATP-activated current.  $V_c$  is the command voltage.

**c** The mean agonist-activated current in response to different concentrations of ATP and BzATP in paired cells. \* Significant difference from ATP, with corresponding  $P$  values given below each set of data.  $n$ , number of patches. **d** Dose response to ATP (filled square) and BzATP (filled circle). Lines through data points are the best fit to the Hill equation,  $r^2 = 0.996$  and  $0.998$  for ATP and BzATP, respectively

respectively ( $P = 0.91$ ). In the second set of experiments, BzATP increased whole-cell current by  $-32.0 \pm 7.29$  pA ( $n = 6$ ). In the presence of KN-62 this was unchanged,  $-27.8 \pm 7.24$  pA ( $P = 0.27$ ).

#### Current Properties and Relative Permeability of ATP-Activated Current

Figure 4a shows typical traces obtained in the absence and presence of  $2$  mM ATP. Addition of ATP to the bath increased whole-cell currents (Fig. 4) ( $P < 0.001$ ). The inward chord conductance under the control circumstance was  $30.2 \pm 2.66$  μS/cm<sup>2</sup> ( $n = 14$ ). On addition of ATP this increased to  $39.7 \pm 3.18$  μS/cm<sup>2</sup>, a mean increase of  $9.53 \pm 0.90$  μS/cm<sup>2</sup>. The ATP-activated point conductance from these 14 cells is shown in Fig. 4c. Conductance and potential demonstrated a significant negative correlation ( $r^2 = -0.86$ ,  $P < 0.05$ ), indicating that the ATP-activated current demonstrated inward rectification. The ATP-activated current was potentiated by 1-min incubation with  $10$  μM ivermectin. Initially, ATP increased the current at  $-100$  mV from  $-710 \pm 216$  to  $-809 \pm 232$  pA ( $n = 7$ ). However, after incubation of the same patches in ivermectin, the current increased from  $-657 \pm 220$  to  $-785 \pm 239$  pA ( $n = 7$ ). The mean ATP-activated current

in the presence of ivermectin, which enhances the activation of P2X<sub>4</sub>, was significantly greater,  $-98.1 \pm 23.2$  vs.  $-127 \pm 23.1$  pA ( $n = 7$ ,  $P = 0.025$ ), in the absence and presence of ivermectin, respectively.

With  $100$  mM NaCl in the bath, the mean  $V_{rev}$  of the ATP-activated current was  $+1.29 \pm 2.01$  mV ( $n = 10$ ). On reducing bath NaCl to  $20$  mM NaCl, the  $V_{rev}$  shifted to  $-24.4 \pm 3.26$  mV ( $P < 0.001$ ), a mean shift of  $-25.6 \pm 2.27$  mV. This corresponded to a cation to anion permeability ratio of  $15.5 \pm 6.75$  (Fig. 5a). Substitution of NaCl for RbCl or CsCl shifted the  $V_{rev}$  by  $+5.65 \pm 1.35$  mV ( $n = 9$ ,  $P = 0.002$ ) and  $+4.22 \pm 1.04$  mV ( $n = 8$ ,  $P = 0.003$ ) with RbCl and CsCl, respectively. LiCl was without effect on  $V_{rev}$ ,  $+1.37 \pm 2.14$  mV ( $n = 8$ ,  $P = 0.52$ ). These shifts corresponded to cation to Na<sup>+</sup> selectivity ratios of  $1.28 \pm 0.07$ ,  $1.22 \pm 0.04$  and  $1.08 \pm 0.10$ , for Rb<sup>+</sup>, Cs<sup>+</sup> and Li<sup>+</sup>, respectively. The  $V_{rev}$  of the ATP-activated current with Na<sup>+</sup> in the pipette and NMDG<sup>+</sup> in the bath was  $-29.4 \pm 1.62$  mV ( $n = 7$ ) (Fig. 5b). This corresponded to an NMDG<sup>+</sup>:Na<sup>+</sup> permeability ratio of  $0.32 \pm 0.02$ . Addition of  $5$  mM Ca<sup>2+</sup> to the extracellular solution shifted the  $V_{rev}$  by  $+5.72 \pm 1.90$  mV ( $n = 7$ ,  $P = 0.017$ ) (Fig. 5c). This corresponded to a Ca<sup>2+</sup>:Na<sup>+</sup> permeability ratio of  $6.56 \pm 2.98$ . These data correspond to a selectivity sequence of Ca<sup>2+</sup> > Rb<sup>+</sup> = Cs<sup>+</sup> > Na<sup>+</sup> = Li<sup>+</sup> > NMDG<sup>+</sup>.

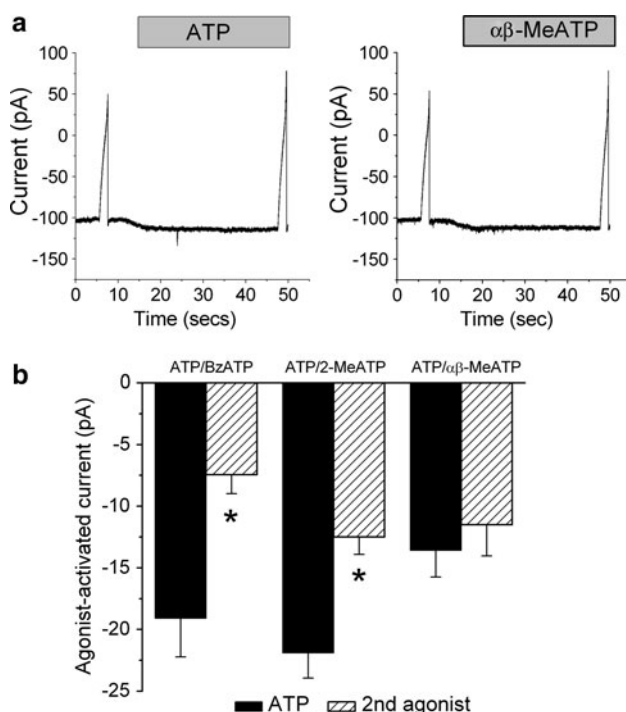


**Fig. 2** Response to different P2X receptor agonists. Clamp potential was held at  $-100$  mV. Under control conditions and in the presence of the agonist a ramp protocol was run between  $-100$  and  $+20$  mV. **a** Typical traces showing the effect of  $500$   $\mu$ M ATP (left) and  $\alpha\beta$ -MeATP (right) in the same cell. **b** Mean agonist-activated current at  $-100$  mV in paired cells exposed to ATP and a second agonist. \* Significant difference from ATP

#### Effect of Extracellular Cations

$Zn^{2+}$  increased the ATP-activated conductance ( $G_{ATP}$ ) ( $n = 10$ ,  $P = 0.004$ ) (Fig. 6). The  $Zn^{2+}$ -mediated enhancement of  $G_{ATP}$  was reversible, with  $G_{ATP}$  returning to pre- $Zn^{2+}$  levels on washout. In the  $Cu^{2+}$  experiments the effect of ATP was attenuated ( $n = 7$ ,  $P = 0.003$ ) (Fig. 6). The  $Cu^{2+}$ -mediated inhibition of  $G_{ATP}$  was reversible, with  $G_{ATP}$  returning to pre- $Cu^{2+}$  levels on washout. With  $0.5$  mM  $Ca^{2+}$  in the bath  $G_{ATP}$  was  $6.24 \pm 0.74$   $\mu$ S/cm<sup>2</sup> ( $n = 16$ ). This was significantly reduced when bath  $Ca^{2+}$  was increased to  $2$  mM ( $P = 0.03$ ) (Fig. 6). However, this reduction in  $G_{ATP}$  was not reversible. Acidification inhibited, while alkalization activated,  $G_{ATP}$  (mean data shown in Table 1).

#### Effect of P2X Activation on Whole-Cell $K^+$ Conductance

Whole-cell potential was clamped at  $-40$  mV and then stepped to between  $+20$  and  $-100$  mV in  $-20$ -mV steps. In control cells at time zero, quinidine inhibited a whole-cell current,  $I_{Quin}$  (Fig. 7a) ( $P < 0.001$ ). The quinidine-sensitive

outward and inward conductances ( $GQ_{out}$  and  $GQ_{in}$ ) were  $7.65 \pm 1.09$  and  $12.2 \pm 1.56$   $\mu$ S/cm<sup>2</sup>, respectively ( $n = 15$ ). The  $V_{rev}$  of  $I_{Quin}$  was  $-41.4 \pm 3.84$  mV (Fig. 7e), consistent with  $K^+$ -selective currents. However,  $I_{Quin}$  decreased after 5 min (Fig. 7b).  $GQ_{out}$  and  $GQ_{in}$  were significantly reduced at  $5.26 \pm 0.60$  and  $7.38 \pm 0.99$   $\mu$ S/cm<sup>2</sup>, respectively ( $n = 15$ ,  $P < 0.001$ ). The  $V_{rev}$  was unchanged,  $-39.16 \pm 4.98$  mV ( $P = 0.46$ ) (Fig. 7e). In a separate population of test cells the responses to quinidine before and after the addition of ATP were determined. The initial  $GQ_{out}$  and  $GQ_{in}$  in the absence of ATP were  $13.2 \pm 2.18$  and  $23.6 \pm 3.73$   $\mu$ S/cm<sup>2</sup>, respectively ( $n = 17$ ). After 5-min exposure to ATP, these were unchanged,  $GQ_{out}$   $9.5 \pm 1.47$  and  $GQ_{in}$   $22.3 \pm 3.50$   $\mu$ S/cm<sup>2</sup> ( $P > 0.12$ ) (Fig. 7f). The  $V_{rev}$  of  $I_{Quin}$  was  $-42.3 \pm 4.07$  and  $-41.8 \pm 6.49$  mV, initially and after 5-min exposure to ATP, respectively ( $P = 0.93$ ) (Fig. 7f). Addition of ATP to the extracellular solution increased the outward and inward conductances by  $8.26 \pm 1.67$  and  $15.7 \pm 2.20$   $\mu$ S/cm<sup>2</sup>, respectively, after 5 min ( $n = 17$ ,  $P < 0.0001$ ) (Fig. 7c). The  $V_{rev}$  of the ATP-activated current was  $-25.7 \pm 4.11$  mV (Fig. 7d). This was significantly depolarized in comparison to the  $V_{rev}$  of  $I_{Quin}$  ( $P = 0.01$ ).

#### Role of P2X Receptors in Volume Regulation

Hypotonic shock elicited two responses, as described previously (Robson and Hunter 1994c). In 29 cells (42%), cell length increased to a peak, with recovery observed when cells were placed back in control Ringer. These were designated “non-RVD” cells (Fig. 8a, lower trace) and represent cells that require  $HCO_3^-$  for regulatory volume decrease (RVD) (Robson and Hunter 1994c). These cells were not considered further in the context of this study. In the remaining 40 cells (58%) cell length increased to a peak, followed by recovery toward the preshock level. These were designated “RVD” cells (Fig. 8a, upper trace). The initial length of the RVD cells was  $21.2 \pm 0.34$   $\mu$ m ( $n = 40$ ). Hypotonic shock increased this by  $0.80 \pm 0.04$   $\mu$ m ( $P < 0.0001$ ), followed by recovery. Steady-state length was  $0.13 \pm 0.05$   $\mu$ m above the preshock level at steady state after volume regulation.

A possible role for extracellular ATP in RVD was examined by exposing cells to ATP/ADP apyrase. Neither the proportion of cells undergoing RVD (64%,  $n = 7$ , Fisher’s exact probability test) nor the initial length of the cells ( $22.4 \pm 0.76$   $\mu$ m,  $n = 7$ , unpaired Student’s *t*-test) was different from control RVD cells. However, ATP/ADP apyrase inhibited RVD in comparison to control cells (unpaired Student’s *t*-test). Figure 8b shows the increase to peak and steady-state length after RVD relative to initial length for apyrase and day-matched controls (control 1).

In a second series of experiments, two types of response were observed in control cells, as described previously,

**Fig. 3** Effect of antagonists on the 500  $\mu$ M ATP-activated current. Cells were held at  $-100$  mV and then exposed to 500  $\mu$ M ATP in the absence and then the presence of the antagonist. This was followed by a second control exposure to ATP after washout of the antagonist. **a-c** Typical whole-cell traces at  $-100$  mV from three different cells in the absence and presence of 100  $\mu$ M suramin, 30 nM TNP-ATP or 10  $\mu$ M PPADS, respectively. *Arrows* indicate when 500  $\mu$ M ATP was added to the bath. **d** Mean ATP-activated currents. \* Significant reduction compared to the first response to ATP. *Black bars* indicate ATP, *hatched bars* indicate ATP plus antagonist and *gray bars* indicate ATP

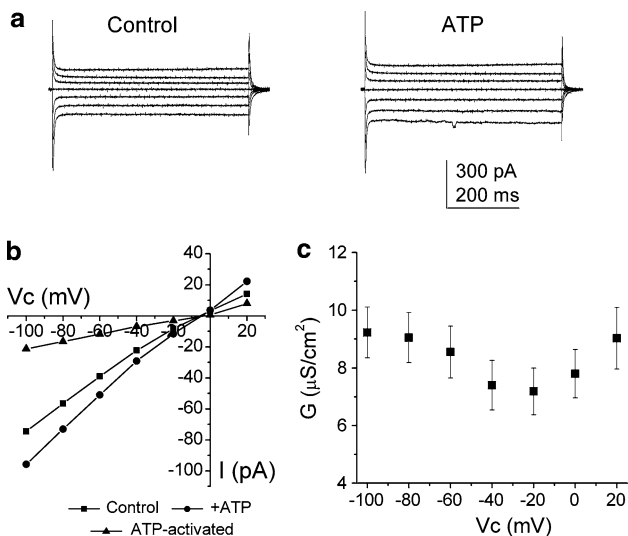
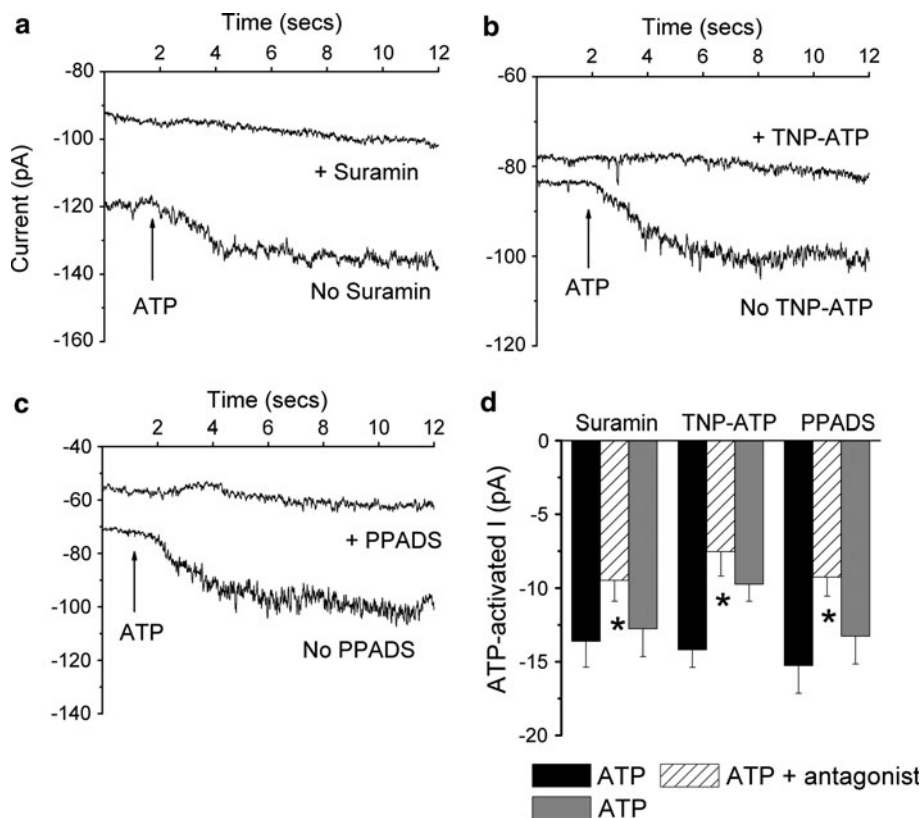


**Fig. 4** Effect of ATP on whole-cell currents. Cells were clamped at  $-40$  mV and then potential stepped to between  $+20$  and  $-100$  mV in  $-20$ -mV steps. **a** Typical traces obtained from the same cell in the absence (*left*) and presence (*right*) of 2 mM ATP. **b** *I-V* curves generated from the traces shown in **a**. *Vc* is the command voltage. **c** Mean point conductance of the ATP-activated currents ( $n = 14$ )

RVD (47%) and non-RVD cells (53%). In RVD cells initial length was  $22.2 \pm 0.46 \mu\text{m}$  ( $n = 22$ ). On exposure to a hypotonic shock, length increased by  $0.66 \pm 0.04 \mu\text{m}$ , to a

peak of  $22.9 \pm 0.48 \mu\text{m}$  ( $P < 0.001$ ), followed by RVD. Length was  $0.06 \pm 0.08 \mu\text{m}$  above the preshock level at steady state after volume regulation. Under the experimental conditions the proportions of cells undergoing RVD were 75% (21) for 100  $\mu$ M suramin, 63% (12) for 10  $\mu$ M PPADS and 61% (14) for 30 nM TNP-ATP. The number of RVD cells was significantly increased for suramin but not PPADS or TNP-ATP (Fisher's exact probability test). The initial lengths of RVD cells were  $22.9 \pm 0.47$  ( $n = 21$ ),  $21.7 \pm 1.06$  and  $22.2 \pm 0.54$  ( $n = 14$ )  $\mu\text{m}$  in the presence of suramin, PPADS and TNP-ATP, respectively. Figure 8b shows the increase to peak and steady-state length after RVD relative to initial length for all experimental conditions. Suramin, TNP-ATP and PPADS all inhibited RVD in comparison to the control circumstance,  $F_{3,65} = 5.57$  (all tested using ANOVA).

**Discussion**

These data provide evidence for the functional expression of a P2X-like current in frog renal proximal tubule cells, P2X<sub>f</sub>. P2X<sub>f</sub> was cation-selective, did not discriminate well between monovalent cations, had a poor permeability to NMDG and was around six times more permeable for Ca<sup>2+</sup> over Na<sup>+</sup>. It was activated by a variety of P2X agonists,

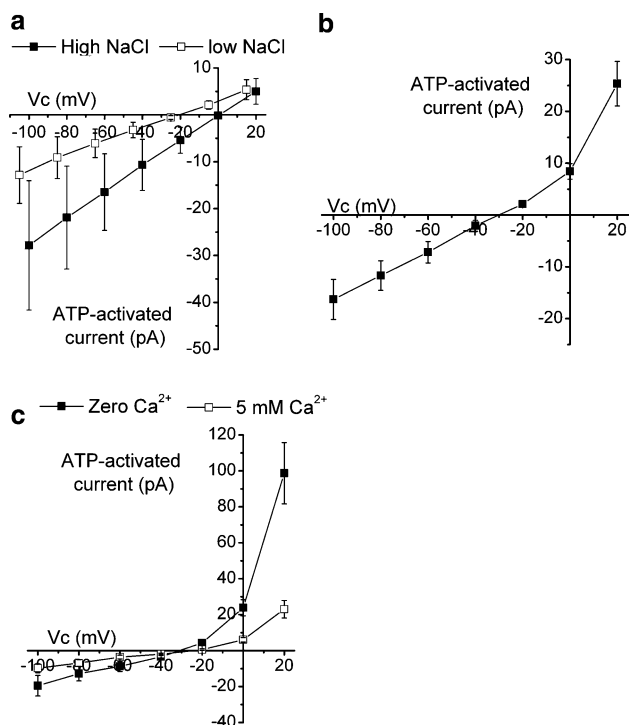


**Fig. 5** Selectivity of ATP-activated current. Cells were clamped at  $-40$  mV and then potential stepped to between  $+20$  and  $-100$  mV in  $-20$ -mV steps.  $V_c$  is the command voltage. **a** Mean currents recorded in high (filled square) or low (open square) NaCl in paired cells ( $n = 10$ ). Note the shift along the  $x$  axis of the low-NaCl data due to junction potential correction. **b** Mean ATP-activated current recorded with NaCl in the pipette and NMDG-Cl in the bath ( $n = 7$ ). **c** Mean ATP-activated currents recorded with bath NMDG-Cl in the absence of  $\text{Ca}^{2+}$  (filled square) or in the presence of  $5$  mM  $\text{Ca}^{2+}$  (open square) in paired cells ( $n = 7$ )

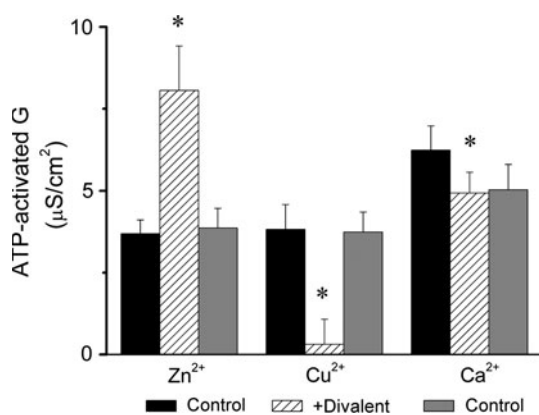


**Fig. 6** Effect of divalent cations on  $G_{\text{ATP}}$ . Cells were clamped at  $-40$  mV and then potential stepped to between  $+20$  and  $-100$  mV in  $-20$ -mV steps. The graph shows the effect of  $\text{Zn}^{2+}$ ,  $\text{Cu}^{2+}$  and  $\text{Ca}^{2+}$ . \* Significantly different response from ATP in the presence of the divalent cation. Black bars indicate ATP, hatched bars indicate ATP plus divalent cation and grey bars indicate ATP

including ATP, BzATP, 2MeSATP and  $\alpha\beta$ -MeATP, and was sensitive to some P2X antagonists. P2X<sub>f</sub> also demonstrated inward rectification, a property shared by some P2X receptors (Evans et al. 1996). These properties are consistent with P2X<sub>f</sub> being attributable to a P2X receptor. However, one difference from P2X receptors was that it was activated only by high concentrations of extracellular ATP,  $100$   $\mu\text{M}$  to  $10$  mM. In contrast, most of the cloned P2X receptors require only micromolar levels of ATP (Torres et al. 1998; Valera et al. 1994; Virginio et al. 1998b), although P2X<sub>7</sub> is activated by high levels of ATP (Rassendren et al. 1997). Consistent with LLC-PK<sub>1</sub> cells (Filipovic et al. 1998), activation of P2X<sub>f</sub> was observed with  $100$   $\mu\text{M}$  ATP, although maximal activation required millimolar levels. The reason for this difference is not clear, but it may reflect the fact that the current study involves an amphibian P2X receptor. Certainly, a study on cloned *Xenopus* P2X<sub>4</sub> also used high concentrations of ATP (Juranka et al. 2001). In addition, frog P2X receptors in aorta require similarly high concentrations of agonists for activation (Knight and Burnstock 1996), with maximal activation not observed with  $3$  mM ATP. Alternatively, it is known that the proximal tubule membrane contains ecto-ATPases that break down ATP (Huang et al. 2006). Therefore, another explanation could be that the ATP in the extracellular solution next to the membrane was at a lower concentration than the bulk solution. The Hill coefficients for ATP and BzATP were similar to other studies (Jiang et al. 2003), with the larger coefficient for ATP suggesting greater cooperativity of binding compared to BzATP. In terms of the in vivo luminal ATP concentration in the proximal tubule, there is a general lack of information, with one study suggesting a maximal concentration of around  $275$  nmol/l in rats (Vekaria et al. 2006). This concentration would not be sufficient to activate P2X<sub>f</sub> and, indeed, is also on the low side for activation of mammalian P2X receptors. However, this concentration reflects the mean in the tubular fluid, and one suggestion is that ATP concentrations closer to the membrane could be much higher. If this is the case, then it is possible that sufficiently high concentrations are reached for activation of both mammalian and amphibian P2X receptors. In addition, as discussed later, it is clear that activation of P2X<sub>f</sub> can impact on the physiological function of the frog renal proximal tubule.

What are the properties of P2X<sub>f</sub>, and how do these compare to the different cloned P2X receptors? Two amphibian cloned receptors have been identified and show 67% homology with rat P2X<sub>4</sub> and P2X<sub>5</sub> (Jensik et al. 2001; Juranka et al. 2001). P2X<sub>f</sub> shows some similarities to these cloned receptors and to some heteromeric mammalian receptors (Table 2). The two amphibian P2X receptors can be activated by levels of ATP, below  $100$   $\mu\text{M}$ . This is

**Table 1** Effect of extracellular pH on the ATP-activated current

$I_{ATP}$ -100 mV (pA)	(n = 9)	$I_{ATP}$ -100 mV (pA)	(n = 9)
pH 7.4	-21.4 ± 2.94	pH 7.4	-19.0 ± 4.03
pH 6.3	-12.2 ± 2.73*	pH 8.3	-30.2 ± 6.45*
pH 7.4	-20.1 ± 4.23	pH 7.4	-24.8 ± 5.01

\* Significant difference from pH 7.4 ( $P < 0.029$ )

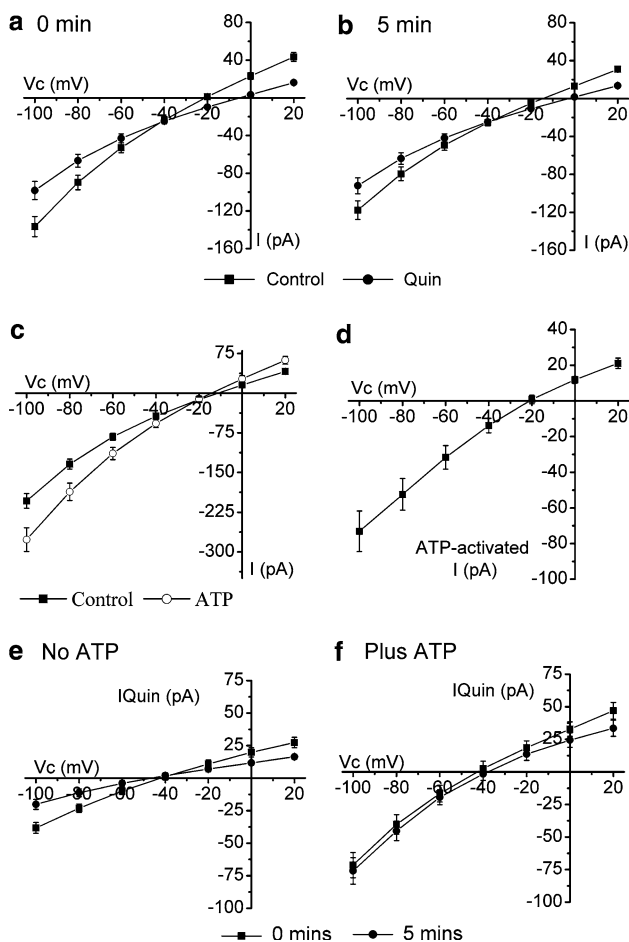


**Fig. 7** Effect of quinidine and ATP on whole-cell currents. Cells were clamped at -40 mV and then potential stepped to between +20 and -100 mV in -20-mV steps.  $V_c$  is the command voltage. **a, b** Mean whole-cell currents recorded in the absence of ATP initially on achieving the whole-cell configuration (**a**) and after 5 min (**b**). In both figures filled square indicates currents recorded in the absence of quinidine, while filled circle indicates currents recorded in the presence of quinidine ( $n = 15$  for all). **c** Effect of addition of extracellular ATP on mean whole-cell current. Filled square, currents recorded in the absence of ATP; open circle, currents recorded after 5-min exposure to ATP ( $n = 17$ ). **d** Mean ATP-activated current. **e, f** Quinidine-sensitive currents in the absence of ATP (**e**) or presence of ATP (**f**). In both graphs filled square indicates currents recorded initially after achieving the whole-cell configuration, while filled circle indicates currents recorded 5 min later

different from  $P2X_f$ , where 100  $\mu$ M ATP was needed for activation. However, as neither study performed a dose response to ATP, a definitive comparison cannot be made.

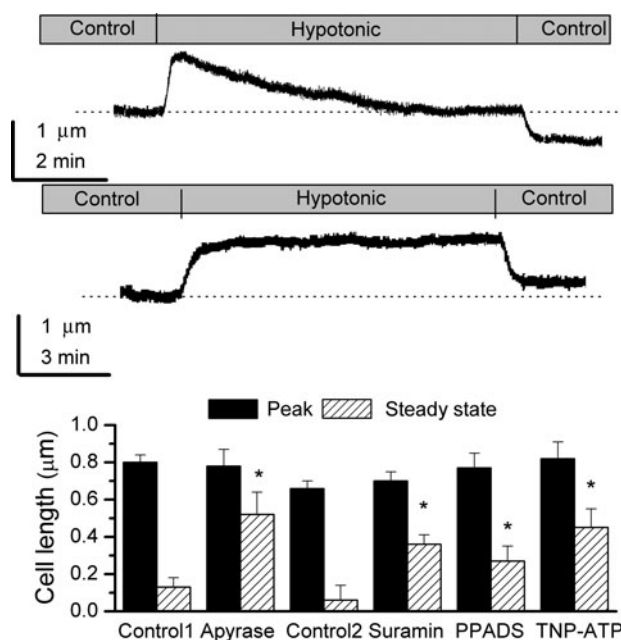


**Fig. 8** Effect of P2X antagonists on RVD. **a** Typical cell length traces showing an RVD cell (upper) and a non-RVD cell (lower). Dotted lines represent the preshock level. **b** Effect of apyrase, suramin, PPADS and TNP-ATP on RVD. Data are expressed relative to control length, with 0 representing the initial preshock level. \* Significant difference from the control circumstance. *Control1* shows day-matched data for the apyrase experiments; *Control2* shows the day-matched data for the suramin, PPADS and TNP-ATP experiments

In divalent free conditions neither cloned  $P2X_f$  receptor demonstrated rapid desensitization on exposure to ATP, similar to  $P2X_f$ . However, although desensitization was not observed with  $P2X_f$  when bath  $Ca^{2+}$  was low, an apparent desensitization was observed when the cells were exposed to 2 mM  $Ca^{2+}$ . Under this circumstance poor recovery of the response to ATP was observed on washout of  $Ca^{2+}$  from the bath. This decrease in the response to ATP during several exposures was not observed with low  $Ca^{2+}$  and is consistent with the  $Ca^{2+}$ -dependent desensitization observed in amphibian  $P2X_f$  receptors. The agonist potency sequence of  $P2X_f$ ,  $ATP = \alpha\beta meATP > BzATP = 2Me-SATP$ , is similar to the frog aorta  $P2X_f$  receptor (Knight and Burnstock 1996). This suggests that  $P2X_f$  is not attributable to  $P2X_7$  (Rassendren et al. 1997), although variations in the response to BzATP are seen at  $P2X_7$  receptors from different species (Fonfria et al. 2008). It is therefore not

**Table 2** Comparison of the properties of P2X<sub>f</sub> with cloned amphibian and mammalian heteromeric receptors

	Amphibian P2X <sub>4</sub>	Amphibian P2X <sub>5</sub>	P2X <sub>2/3</sub>	P2X <sub>1/4</sub>	P2X <sub>1/5</sub>	P2X <sub>4/6</sub>	References
Agonist potency		X	◆	◆	◆	X	Jensik et al. (2001)
Suramin		>	>	>	>	◆ 40%	Juranka et al. (2001) Le et al. (1998)
PPADS	◆	>	>	>	>	◆	Le et al. (1999)
TNP-ATP			>	>	>		Liu et al. (2001)
Zn <sup>2+</sup>			◆			◆	Nicke et al. (2005)
Ca <sup>2+</sup>		◆	◆		X		Stoop et al. (1997)
pH			X		◆	◆	Virginio et al. (1998a) Wildman et al. (1998)

Percentages indicate percentage inhibition values close to those observed for P2X<sub>f</sub>

◆, Similarity to P2X<sub>f</sub>; X, difference; >, higher sensitivity; blank, not known

possible to absolutely rule out P2X<sub>f</sub> being attributable to a P2X<sub>7</sub>-like receptor, although the P2X<sub>7</sub> antagonists KN-62 and BBG were without effect on P2X<sub>f</sub> (Humphreys et al. 1998; Jiang et al. 2000). P2X<sub>f</sub> was sensitive to 100 μM suramin, 10 μM PPADS and 30 nM TNP-ATP (30%, 44% and 34% inhibition, respectively). This sensitivity to PPADS is similar to amphibian P2X<sub>4</sub> (50% inhibition) (Juranka et al. 2001) and P2X<sub>4/6</sub> (40% inhibition) (Le et al. 1998), although it is different from the bullfrog P2X receptor, which is completely blocked by both 100 μM suramin and PPADS (Jensik et al. 2001). The sensitivity to PPADS was similar to amphibian P2X<sub>4</sub> and P2X<sub>4/6</sub>. TNP-ATP is a potent inhibitor of P2X<sub>1/5</sub>, P2X<sub>1/4</sub> and P2X<sub>2/3</sub> (Le et al. 1999; Nicke et al. 2005; Virginio et al. 1998b), with ~80% inhibition observed with 30 nM. This is higher than the sensitivity of P2X<sub>f</sub>. Like P2X<sub>f</sub>, the bullfrog cloned receptor also shows inhibition by Ca<sup>2+</sup> (Jensik et al. 2001). P2X<sub>f</sub> was potentiated by ivermectin, which is known to enhance activation of P2X<sub>4</sub> (Priel and Silberberg 2004) and was also potentiated by extracellular Zn<sup>2+</sup> and inhibited by extracellular Cu<sup>2+</sup> and H<sup>+</sup>.

Overall, P2X<sub>f</sub> would appear to share greatest similarity with P2X<sub>2/3</sub> or P2X<sub>4/6</sub>, although its properties are not entirely consistent with these heteromeric P2X receptors. Given the fact that previous expression studies have shown the presence of P2X<sub>1</sub>, P2X<sub>4</sub>, P2X<sub>5</sub> and P2X<sub>6</sub> in the renal proximal tubule, it is likely that P2X<sub>f</sub> represents a P2X<sub>4/6</sub>-like P2X receptor.

P2X<sub>f</sub> is clearly a native proximal tubule P2X-like receptor, and on activation it would be expected to lead to an influx of Ca<sup>2+</sup> into the cell. However, the magnitude of the P2X<sub>f</sub>-mediated currents was small. In comparison to P2X receptor expression studies this is to be expected as in those studies the magnitude of the P2X currents reflects the fact that the channels have been overexpressed. Looking at studies of native P2X receptor currents provides a variable

picture in terms of current magnitude. In LLC-PK<sub>1</sub> cells, currents were on the order of a few hundred picoamperes (Filipovic et al. 1998). In contrast, studies in neurons, airway ciliated cells and Leydig cells show small P2X-mediated currents, similar to P2X<sub>f</sub> (Chaves et al. 2006; Ma et al. 2006; Mori et al. 2001). It is clear, therefore, that physiologically relevant P2X native currents can be small. What is the physiological role of P2X<sub>f</sub> in the renal proximal tubule? The data presented in the current study suggest that P2X<sub>f</sub> plays an important role in volume regulation and K<sup>+</sup> channel activation.

Frog proximal tubule cells have the ability to regulate their volume in response to cell swelling, RVD (Robson and Hunter 1994c). Such volume regulation plays an important role in diverse cellular process such as cell growth and proliferation, osmoregulation and cellular metabolism. There is a clear role for P2 activation in regulating proximal tubule cell proliferation (Lee and Han 2006), while a role for P2 receptor activation in RVD in hepatocytes has been proposed (Wang et al. 1996). This suggests that P2 receptors and volume regulation may be important for normal cell function. Previous work in frog proximal cells has demonstrated a role for K<sup>+</sup> and Cl<sup>-</sup> channels in RVD (Robson and Hunter 1994c, 2005). Whole-cell patch-clamp experiments have identified barium-sensitive K<sup>+</sup> and DIDS-sensitive Cl<sup>-</sup> currents that are volume sensitive (Robson and Hunter 1994a, 2005). Unpublished studies demonstrate that quinidine-sensitive K<sup>+</sup> currents are also volume-sensitive, with quinidine-sensitive conductance reduced in the presence of a hypertonic bath solution (19.2 ± 4.38 vs. 7.31 ± 1.46 μS/cm<sup>2</sup> in the presence of control and hypertonic solutions, respectively, n = 12 for each group). For the Cl<sup>-</sup> channels volume activation is mediated by protein kinase C (PKC) (Robson and Hunter 1994a). The mechanism underlying volume regulation of the K<sup>+</sup> currents has not been

elucidated but does not appear to involve PKC. In addition, RVD is inhibited in the absence of extracellular  $\text{Ca}^{2+}$ , consistent with a  $\text{Ca}^{2+}$  influx pathway playing a critical role (Robson and Hunter 1994c). The specific mechanism by which  $\text{Ca}^{2+}$  enters the renal proximal is unknown; however, a number of candidates have been proposed. One of these is stretch-activated,  $\text{Ca}^{2+}$ -permeable cation channels (SACs), as the SAC inhibitor gadolinium ( $\text{Gd}^{3+}$ ) blocks RVD (Robson and Hunter 1994c) and two  $\text{Gd}^{3+}$  and volume-sensitive cation conductances have been identified in these cells (Robson and Hunter 1994b). However, subsequent work has indicated that the volume-sensitive  $\text{Cl}^-$  channels are also inhibited by  $\text{Gd}^{3+}$  (Robson and Hunter 1994a). Therefore, the effect of  $\text{Gd}^{3+}$  on RVD could simply reflect inhibition of  $\text{Cl}^-$  efflux rather than  $\text{Ca}^{2+}$  influx. A second possibility is that, on cell swelling, there is release of ATP from the cells, with ATP subsequently leading to  $\text{Ca}^{2+}$  influx via the activation of P2X receptors. This is supported by the current study, which demonstrated that in the presence of apyrase RVD was inhibited, suggesting that the release and presence of ATP are important in initiating volume regulation. RVD was also inhibited by the P2X antagonists suramin, TNP-ATP and PPADS. This supports a role for P2X receptor activation in RVD. The degree of inhibition of RVD was similar to that observed with  $\text{P2X}_f$ .

These data support a role for  $\text{P2X}_f$  activation in RVD and suggest that it may provide the  $\text{Ca}^{2+}$  influx pathway. This influx of  $\text{Ca}^{2+}$  would be expected to activate downstream efflux pathways, such as the  $\text{K}^+$  and  $\text{Cl}^-$  channels described earlier. A clear link exists to activation of the  $\text{Cl}^-$  channels as this is PKC-mediated. For the activation of  $\text{K}^+$  channels a rise in intracellular  $\text{Ca}^{2+}$  could directly activate channels or work indirectly via  $\text{Ca}^{2+}$ -dependent signalling systems. The whole-cell  $\text{K}^+$  current data described here suggest that  $\text{P2X}_f$  plays an important role in the activation of quinidine-sensitive  $\text{K}^+$  channels previously observed in the cells. In the absence of extracellular ATP, whole-cell quinidine-sensitive  $\text{K}^+$  currents decreased over 5 min. However, in the presence of extracellular ATP this rundown was absent, indicating that extracellular ATP was able to inhibit the rundown process. The  $V_{\text{rev}}$  of the quinidine-sensitive currents, around  $-40$  mV, suggests that the  $\text{K}^+$  channel regulated by extracellular ATP was a previously identified  $\text{K}^+$  conductance (Robson and Hunter 1997). The total ATP activated current demonstrated inward rectification, similar to  $\text{P2X}_f$ . Interestingly, the  $V_{\text{rev}}$  of the total ATP-activated current was more positive than the  $\text{K}^+$  currents but more negative than the  $V_{\text{rev}}$  for  $\text{P2X}_f$ . This suggests that at least part of the ATP-activated current may reflect activation of  $\text{K}^+$ -selective channels. Activation of  $\text{K}^+$  channels via P2X receptor activation has been observed in rat osteoclasts and toad gastric smooth muscle

cells (Weidema et al. 1997; Zou et al. 2001), with  $\text{P2Y}_2$ -mediated inhibition of  $\text{K}^+$  channels in the mouse cortical collecting duct (Lu et al. 2000).

In conclusion, the current study provides the first report of a native P2X receptor in renal proximal tubule cells. The receptor,  $\text{P2X}_f$ , was cation-selective, did not discriminate between cations and was  $\text{Ca}^{2+}$ -permeable.  $\text{P2X}_f$  was activated by the purines  $\text{ATP} = \alpha\beta\text{meATP} > \text{BzATP} = 2\text{MeSATP}$ , did not demonstrate fast desensitization and was inhibited by suramin, PPADS and TNP-ATP.  $\text{P2X}_f$ -mediated currents were enhanced in the presence of  $\text{Zn}^{2+}$  or ivermectin and inhibited in the presence of  $\text{Cu}^{2+}$  or on acidification. These properties are consistent with  $\text{P2X}_f$  being attributable to a P2X receptor and suggest that  $\text{P2X}_f$  may be attributable to a heteromeric receptor, with  $\text{P2X}_{4/6}$  a possible candidate. The evidence presented suggests that activation of  $\text{P2X}_f$  plays a role in the regulation of cell volume and  $\text{K}^+$  channels in frog renal proximal tubule cells.

**Acknowledgement** This work was funded by the Wellcome Trust. J. P. D. was supported by a University of Sheffield studentship.

**Open Access** This article is distributed under the terms of the Creative Commons Attribution Noncommercial License which permits any noncommercial use, distribution, and reproduction in any medium, provided the original author(s) and source are credited.

## References

- Bailey MA (2004) Inhibition of bicarbonate reabsorption in the rat proximal tubule by activation of luminal  $\text{P2Y}_1$  receptors. *Am J Physiol Renal Physiol* 287:F789–F796
- Bailey MA, Imbert-Teboul M, Turner C, Srai SK, Burnstock G, Unwin RJ (2001) Evidence for basolateral  $\text{P2Y}_6$  receptors along the rat proximal tubule: functional and molecular characterization. *J Am Soc Nephrol* 12:1640–1647
- Bouyer P, Paulais M, Coughnon M, Hulin P, Anagnostopoulos T, Planelles G (1998) Extracellular ATP raises cytosolic calcium and activates basolateral chloride conductance in *Necturus* proximal tubule. *J Physiol* 510:535–548
- Burnstock G, Kennedy C (1985) Is there a basis for distinguishing two types of P2-purinoceptor? *Gen Pharmacol* 16:433–440
- Cha SH, Sekine T, Endou H (1998) P2 purinoceptor localization along rat nephron and evidence suggesting existence of subtypes  $\text{P2Y}_1$  and  $\text{P2Y}_2$ . *Am J Physiol Renal Physiol* 274:F1006–F1014
- Chan CM, Unwin RJ, Bardini M, Oglesby IB, Ford APDW, Townsend-Nicholson A, Burnstock G (1998) Localization of  $\text{P2X}_1$  purinoceptors by autoradiography and immunohistochemistry in rat kidneys. *Am J Physiol Renal Physiol* 274:F799–F804
- Chaves LAP, Pontelli EP, Varanda WA (2006) P2X receptors in mouse Leydig cells. *Am J Physiol Cell Physiol* 290:C1009–C1017
- Evans RJ, Lewis C, Virginio C, Lundstrom K, Buell G, Surprenant A, North RA (1996) Ionic permeability of, and divalent cation effects on, two ATP-gated cation channels ( $\text{P2X}$  receptors) expressed in mammalian cells. *J Physiol* 497:413–422

- Filipovic DM, Adebajo OA, Zaidi M, Reeves WB (1998) Functional and molecular evidence for P2X receptors in LLC-PK1 cells. *Am J Physiol Renal Physiol* 274:F1070–F1077
- Fonfria E, Levy DS, Goodwin JA, Roman S, Smith GD, Condreay JP, Michel AD (2008) Cloning and pharmacological characterization of the guinea pig P2X7 receptor orthologue. *Br J Pharmacol* 153:544–556
- Guo C, Masin M, Qureshi OS, Murrell-Lagnado RD (2007) Evidence for functional P2X4/P2X7 heteromeric receptors. *Mol Pharmacol* 72:1447–1456
- Hamill OP, Marty A, Neher E, Sakmann B, Sigworth FJ (1981) Improved patch-clamp techniques for high-resolution current recording from cells and cell-free membrane patches. *Pflügers Arch* 391:85–100
- Huang DY, Vallon V, Zimmermann H, Koszalka P, Schrader J, Osswald H (2006) Ecto-5'-nucleotidase (cd73)-dependent and -independent generation of adenosine participates in the mediation of tubuloglomerular feedback in vivo. *Am J Physiol Renal Physiol* 291:F282–F288
- Humphreys BD, Virginio C, Surprenant A, Rice J, Dubyak GR (1998) Isoquinolines as antagonists of the P2X7 nucleotide receptor: high selectivity for the human versus rat receptor homologues. *Mol Pharmacol* 54:22–32
- Hunter M (1989) Isolation of single proximal cells from frog kidneys. *J Physiol* 416:13P
- Jensen MEJ, Odgaard E, Christensen MH, Praetorius HA, Leipziger J (2007) Flow-induced  $[Ca^{2+}]_i$  increase depends on nucleotide release and subsequent purinergic signaling in the intact nephron. *J Am Soc Nephrol* 18:2062–2070
- Jensik PJ, Holbirt D, Collard MW, Cox TC (2001) Cloning and characterization of a functional P2X receptor from larval bullfrog skin. *Am J Physiol Cell Physiol* 281:C954–C962
- Jiang L-H, Mackenzie AB, North RA, Surprenant A (2000) Brilliant blue G selectively blocks ATP-gated rat P2X7 receptors. *Mol Pharmacol* 58:82–88
- Jiang L-H, Kim M, Spelta V, Bo X, Surprenant A, North RA (2003) Subunit arrangement in P2X receptors. *J Neurosci* 23:8903–8910
- Juranka PF, Haghighi AP, Gaertner T, Cooper E, Morris CE (2001) Molecular cloning and functional expression of *Xenopus laevis* oocyte ATP-activated P2X4 channels. *Biochim Biophys Acta* 1512:111–124
- Knight GE, Burnstock G (1996) The effects of purine compounds on the isolated aorta of the frog *Rana temporaria*. *Br J Pharmacol* 117:873–878
- Laycock S, Taylor HC, Haigh C, Lee AT, Cooper GJ, Ong ACM, Robson L (2009) A novel dephosphorylation-activated conductance in a mouse renal collecting duct cell line. *Exp Physiol* 94:914–927
- Le K-T, Babinski K, Seguela P (1998) Central P2X4 and P2X6 channel subunits coassemble into a novel heteromeric ATP receptor. *J Neurosci* 18:7152–7159
- Le K-T, Boue-Grabot E, Archambault V, Seguela P (1999) Functional and biochemical evidence for heteromeric ATP-gated channels composed of P2X1 and P2X5 subunits. *J Biol Chem* 274:15415–15419
- Lee YJ, Han HJ (2006) Role of ATP in DNA synthesis of renal proximal tubule cells: involvement of calcium, MAPKs, and CDKs. *Am J Physiol Renal Physiol* 291:F98–F106
- Lee YJ, Park SH, Han HJ (2005) ATP stimulates  $Na^+$ -glucose cotransporter activity via cAMP and p38 MAPK in renal proximal tubule cells. *Am J Physiol Cell Physiol* 289:C1268–C1276
- Leipziger J, Unwin RJ (2003) Purinergic receptors in the kidney. In: Schwiebert EM (ed) Purinergic receptors and signalling. Academic Press, San Diego, pp 369–394
- Lewis C, Neidhart S, Holy C, North RA, Buell G, Surprenant A (1995) Coexpression of P2X2 and P2X3 receptor subunits can account for ATP-gated currents in sensory neurons. *Nature* 377:432–435
- Liu M, King BF, Dunn PM, Rong W, Townsend-Nicholson A, Burnstock G (2001) Coexpression of P2X3 and P2X2 receptor subunits in varying amounts generates heterogeneous populations of P2X receptors that evoke a spectrum of agonist responses comparable to that seen in sensory neurons. *J Pharmacol Exp Ther* 296:1043–1050
- Liu R, Bell PD, Peti-Peterdi J, Kovacs G, Johansson A, Persson AEG (2002) Purinergic receptor signaling at the basolateral membrane of macula densa cells. *J Am Soc Nephrol* 13:1145–1151
- Lu M, MacGregor GG, Wang W, Giebisch G (2000) Extracellular ATP inhibits the small-conductance K channel on the apical membrane of the cortical collecting duct from mouse kidney. *J Gen Physiol* 116:299–310
- Ma W, Korngreen A, Weil S, Cohen EB-T, Priel A, Kuzin L, Silberberg SD (2006) Pore properties and pharmacological features of the P2X receptor channel in airway ciliated cells. *J Physiol* 571:503–517
- McCoy DE, Taylor AL, Kudlow BA, Karlson K, Slattery MJ, Schwiebert LM, Schwiebert EM, Stanton BA (1999) Nucleotides regulate  $NaCl$  transport in mIMCD-K2 cells via P2X and P2Y purinergic receptors. *Am J Physiol Renal Physiol* 277:F552–F559
- Mori M, Heuss C, Gähwiler BH, Gerber U (2001) Fast synaptic transmission mediated by P2X receptors in CA3 pyramidal cells of rat hippocampal slice cultures. *J Physiol* 535:115–123
- Mounfield PR, Robson L (1998) The role of  $Ca^{2+}$  in volume regulation induced by  $Na^+$ -coupled alanine uptake in single proximal tubule cells isolated from frog kidney. *J Physiol* 510:145–153
- Nicke A, Kerschensteiner D, Soto F (2005) Biochemical and functional evidence for heteromeric assembly of P2X1 and P2X4 subunits. *J Neurochem* 92:925–933
- North RA, Barnard EA (1997) Nucleotide receptors. *Curr Opin Neurobiol* 7:346–357
- Pochynyuk O, Bugaj V, Rieg T, Insel PA, Mironova E, Vallon V, Stockand JD (2008) Paracrine regulation of the epithelial  $Na^+$  channel in the mammalian collecting duct by purinergic P2Y2 receptor tone. *J Biol Chem* 283:36599–36607
- Priel A, Silberberg SD (2004) Mechanism of ivermectin facilitation of human P2X4 receptor channels. *J Gen Physiol* 123:281–293
- Radford KM, Virginio C, Surprenant A, North RA, Kawashima E (1997) Baculovirus expression provides direct evidence for heteromeric assembly of P2X2 and P2X3 receptors. *J Neurosci* 17:6529–6533
- Rassendren F, Buell GN, Virginio C, Collo G, North RA, Surprenant A (1997) The permeabilizing ATP receptor, P2X7. Cloning and expression of a human cDNA. *J Biol Chem* 272:5482–5486
- Robson L, Hunter M (1994a) Role of cell volume and protein kinase C in regulation of a  $Cl^-$  conductance in single proximal tubule cells of *Rana temporaria*. *J Physiol* 480:1–7
- Robson L, Hunter M (1994b) Volume-activated, gadolinium-sensitive whole-cell currents in single proximal cells of frog kidney. *Pflügers Arch* 429:98–106
- Robson L, Hunter M (1994c) Volume regulatory responses in frog isolated proximal cells. *Pflügers Arch* 428:60–68
- Robson L, Hunter M (1997) Two  $K^+$ -selective conductances in single proximal tubule cells isolated from frog kidney are regulated by ATP. *J Physiol* 500:605–616
- Robson L, Hunter M (2005) Mechanisms underlying regulation of a barium-sensitive  $K^+$  conductance by ATP in single proximal tubule cells isolated from frog kidney. *J Membr Biol* 204:39–47
- Silva GB, Garvin JL (2009) Extracellular ATP inhibits transport in medullary thick ascending limbs: role of P2X receptors. *Am J Physiol Renal Physiol* 297:F1168–F1173

- Solini A, Santini E, Chimenti D, Chiozzi P, Pratesi F, Cuccato S, Falzoni S, Lupi R, Ferrannini E, Pugliese G, Virgilio FD (2007) Multiple P2X receptors are involved in the modulation of apoptosis in human mesangial cells: evidence for a role of P2X4. *Am J Physiol Renal Physiol* 292:F1537–F1547
- Stoop R, Surprenant A, North RA (1997) Different sensitivities to pH of ATP-induced currents at four cloned P2X receptors. *J Neurophysiol* 78:1837–1840
- Takeda M, Kobayashi M, Endou H (1998) Establishment of a mouse clonal early proximal tubule cell line and outer medullary collecting duct cells expressing P2 purinoceptors. *Biochem Mol Biol Int* 44:657–664
- Torres GE, Haines WR, Egan TM, Voigt MM (1998) Co-expression of P2X1 and P2X5 receptor subunits reveals a novel ATP-gated ion channel. *Mol Pharmacol* 54:989–993
- Torres GE, Egan TM, Voigt MM (1999) Hetero-oligomeric assembly of P2X receptor subunits. Specificities exist with regard to possible partners. *J Biol Chem* 274:6653–6659
- Valera S, Hussy N, Evans RJ, Adami N, North RA, Surprenant A, Buell G (1994) A new class of ligand-gated ion channel defined by P2x receptor for extracellular ATP. *Nature* 371:516–519
- Vekaria RM, Unwin RJ, Shirley DG (2006) Intraluminal ATP concentrations in rat renal tubules. *J Am Soc Nephrol* 17:1841–1847
- Virginio C, North RA, Surprenant A (1998a) Calcium permeability and block at homomeric and heteromeric P2X2 and P2X3 receptors, and P2X receptors in rat nodose neurons. *J Physiol* 510:27–35
- Virginio C, Robertson G, Surprenant A, North RA (1998b) Trinitrophenyl-substituted nucleotides are potent antagonists selective for P2X1, P2X3, and heteromeric P2X2/3 receptors. *Mol Pharmacol* 53:969–973
- Wang CZ, Namba N, Gono T, Inagaki N, Seino S (1996) Cloning and pharmacological characterization of a fourth P2X receptor subtype widely expressed in brain and peripheral tissues including various endocrine tissues. *Biochem Biophys Res Commun* 220:196–202
- Weidema AF, Barbera J, Dixon SJ, Sims SM (1997) Extracellular nucleotides activate non-selective cation and Ca<sup>2+</sup>-dependent K<sup>+</sup> channels in rat osteoclasts. *J Physiol* 503:303–315
- Wildman SS, King BF, Burnstock G (1998) Zn<sup>2+</sup> modulation of ATP-responses at recombinant P2X2 receptors and its dependence on extracellular pH. *Br J Pharmacol* 123:1214–1220
- Wildman SSP, Marks J, Turner CM, Yew-Booth L, Peppiatt-Wildman CM, King BF, Shirley DG, Wang W, Unwin RJ (2008) Sodium-dependent regulation of renal amiloride-sensitive currents by apical P2 receptors. *J Am Soc Nephrol* 19:731–742
- Wildman SSP, Boone M, Peppiatt-Wildman CM, Contreras-Sanz A, King BF, Shirley DG, Deen PMT, Unwin RJ (2009) Nucleotides downregulate aquaporin 2 via activation of apical P2 receptors. *J Am Soc Nephrol* 20:1480–1490
- Xia S-L, Wang L, Cash MN, Teng X, Schwalbe RA, Wingo CS (2004) Extracellular ATP-induced calcium signaling in mIMCD-3 cells requires both P2X and P2Y purinoceptors. *Am J Physiol Renal Physiol* 287:F204–F214
- Zhang Y, Sanchez D, Gorelik J, Klenerman D, Lab M, Edwards C, Korchev Y (2007) Basolateral P2X4-like receptors regulate the extracellular ATP-stimulated epithelial Na<sup>+</sup> channel activity in renal epithelia. *Am J Physiol Renal Physiol* 292:F1734–F1740
- Zou H, Ugur M, Drummond RM, Singer JJ (2001) Coupling of a P2Z-like purinoceptor to a fatty acid-activated K<sup>+</sup> channel in toad gastric smooth muscle cells. *J Physiol* 534:59–70